

## Article

# Synthesis of a New Dinuclear Ag(I) Complex with Asymmetric Azine Type Ligand: X-ray Structure and Biological Studies

Mezna Saleh Altowyan <sup>1</sup>, Saied M. Soliman <sup>2,\*</sup>, Dhuha Al-Wahaib <sup>3</sup>, Assem Barakat <sup>4</sup>,  
Ali Eldissouky Ali <sup>2,\*</sup> and Hemmat A. Elbadawy <sup>2,\*</sup>

<sup>1</sup> Department of Chemistry, College of Science, Princess Nourah bint Abdulrahman University, P.O. Box 84428, Riyadh 11671, Saudi Arabia

<sup>2</sup> Chemistry Department, Faculty of Science, Alexandria University, P.O. Box 426, Alexandria 21321, Egypt

<sup>3</sup> Chemistry Department, Faculty of Science, Kuwait University, Kuwait 13060, Kuwait

<sup>4</sup> Department of Chemistry, College of Science, King Saud University, P.O. Box 2455, Riyadh 11451, Saudi Arabia

\* Correspondence: saied1soliman@yahoo.com (S.M.S.); alioldissouky@alexu.edu.eg (A.E.A.); hemmatabdelfattah@alexu.edu.eg (H.A.E.)

**Abstract:** Aspects of the molecular and supramolecular structure of the new dinuclear  $[\text{Ag}(\text{L})(\text{NO}_3)]_2$  complex, where L is 2-((E)-(((E)-1-(thiazol-2-yl)ethylidene)hydrazono)methyl)phenol, were discussed. The complex was crystallized in the monoclinic crystal system and  $P2_1/n$  space group. The unit cell parameters are  $a = 10.3274(2)$  Å,  $b = 11.4504(3)$  Å,  $c = 12.7137(3)$  Å and  $\beta = 108.2560(10)^\circ$ . The asymmetric unit comprised one  $[\text{Ag}(\text{L})(\text{NO}_3)]$  formula in which the azine and nitrate ligand groups act as NN- and OO-bidentate chelates, respectively. The coordination environment of the Ag(I) is completed by one weak Ag-O bond with another  $[\text{Ag}(\text{L})(\text{NO}_3)]$  unit, leading to the dinuclear formula  $[\text{Ag}(\text{L})(\text{NO}_3)]_2$ . This was clearly revealed by Hirshfeld analysis. Additionally, the Ag...C, O...H and C...C intermolecular interactions played an important role in the molecular packing of the studied complex. The antimicrobial, antioxidant and cytotoxic activities of the  $[\text{Ag}(\text{L})(\text{NO}_3)]_2$  complex and the free ligand (L) were discussed. While the  $[\text{Ag}(\text{L})(\text{NO}_3)]_2$  complex showed very weak antioxidant activity, the results of the antifungal and cytotoxic activities were promising. The inhibition zone diameters (IZD) and the minimum inhibitory concentration (MIC) values were determined to be 31 mm and 20 µg/mL, respectively, against *A. fumigatus*, which is compared to 17 mm and 156 µg/mL, respectively, for the positive control Ketoconazole. Generally, the Ag(I) complex has better antimicrobial activities than the free ligand against all microbes except for *S. aureus*, where the free ligand has higher activity. Additionally, the  $\text{IC}_{50}$  value against colon carcinoma (HCT-116 cell line) was determined to be  $12.53 \pm 0.69$  µg/mL, which is compared to  $5.35 \pm 0.49$  µg/mL for *cis*-platin. Additionally, the Ag(I) complex displays better cytotoxicity than the free ligand (L) ( $242.92 \pm 8.12$  µg/mL).

**Keywords:** asymmetric azine; silver(I); Hirshfeld; antimicrobial; anticancer



**Citation:** Altowyan, M.S.; Soliman, S.M.; Al-Wahaib, D.; Barakat, A.; Ali, A.E.; Elbadawy, H.A. Synthesis of a New Dinuclear Ag(I) Complex with Asymmetric Azine Type Ligand: X-ray Structure and Biological Studies. *Inorganics* **2022**, *10*, 209. <https://doi.org/10.3390/inorganics10110209>

Academic Editor: Isabel Correia

Received: 11 October 2022

Accepted: 8 November 2022

Published: 15 November 2022

**Publisher's Note:** MDPI stays neutral with regard to jurisdictional claims in published maps and institutional affiliations.



**Copyright:** © 2022 by the authors. Licensee MDPI, Basel, Switzerland. This article is an open access article distributed under the terms and conditions of the Creative Commons Attribution (CC BY) license (<https://creativecommons.org/licenses/by/4.0/>).

## 1. Introduction

The search for novel drugs for the treatment of diseases such as cancers and antibiotic-resistant microbes is still a challenge, and much effort has been devoted to the discovery of new chemotherapeutic agents. Transition metal complexes are continuously designed, synthesized, and assessed against different targets [1–5]. For example, *cis*-platin is used as an anticancer drug, although it still has limitations due to resistance and significant side effects [6]. This disadvantage encouraged many scientists to search for alternative transition metal complexes for different purposes [7]. Silver(I) complexes play a significant role in the treatment of many diseases such as tumors and bacterial infections [8–15]. The optimism surrounding silver-based drugs is due to their higher drug-tolerance profiles and higher selectivity to cancer cells rather than the non-cancerous cells compared to other

metal complexes. These potential benefits make this area of research important and create the need for further exploration.

One important class of chelating ligands in coordination chemistry is Schiff bases, which are well known and have become important molecules in pharmaceutical and medicinal fields. They exhibit many biological effects, including anti-fungal [16,17], antibacterial [18], herbicidal [19], anti-HIV [16] antitubercular [20], anti-inflammatory [21] and anti-tumor effects [22]. Coordination between the metal and chelating ligands creates a new product with enhanced therapeutic efficiency [23–25]. Understanding and discovering the functions of metal ions in disease treatment is still a challenge in medicinal inorganic and bioinorganic chemistry [26]. In many cases, the donor sequence of the chelating ligands and the identity of the metal play a crucial role in pharmacological activity [27,28]. The thiazole-based Schiff base ligands and their analogues are an important class of chelating ligands in coordination chemistry [29]. The cytotoxic properties of some silver(I) complexes of Schiff bases derived from thiazole and pyrazine scaffolds were reported by X.-J. Tan et al. [30]. Additionally, Ag(I) thiazole-based coordination polymers have interesting photophysical properties [31]. Recently, our research group reported the synthesis of some Ag(I) complexes with symmetric azine-type ligands and explored their molecular, supramolecular and biological aspects [32–34].

Herein, we reported the synthesis, structural and biological evaluation of a new dinuclear Ag(I) complex with the asymmetric azine-type ligand shown in Figure 1. The new Ag(I) metal complex was evaluated for biological efficacy against different targets including anticancer, antimicrobial and antioxidant reactivities.

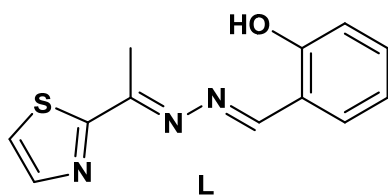
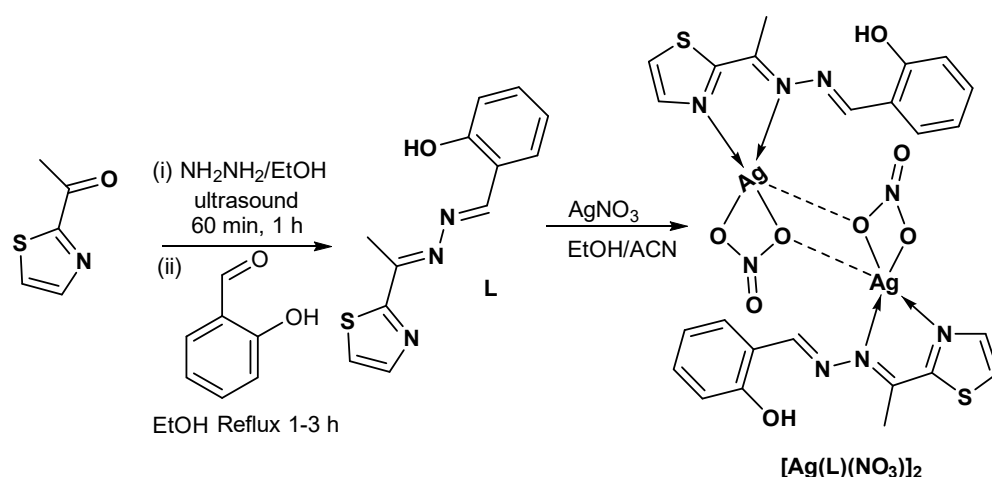


**Figure 1.** Structure of the asymmetric azine ligand.

## 2. Results and Discussion

### 2.1. Synthesis and Characterizations

In our previous work, we examined the reaction of a number of hydrazones and hydrazides with Ag(I) salts [32–34]. Unexpectedly, these reactions proceeded to the formation of the corresponding azine, affording the Ag(I)-azine complexes as final products. Conversely, the reaction of AgNO<sub>3</sub> with the asymmetric azine ligand **L** proceeded without hydrolysis and afforded the dinuclear [Ag(L)(NO<sub>3</sub>)<sub>2</sub>] complex with high yield (Scheme 1). The product was characterized using elemental analysis, FTIR and XPS spectroscopic techniques, and then its structure was unambiguously determined with the aid of single-crystal X-ray diffraction. The FTIR spectral band corresponding to the  $\nu_{C=N}$  stretching vibration appeared at 1615 cm<sup>-1</sup> in case of the [Ag(L)(NO<sub>3</sub>)<sub>2</sub>] complex, while it appeared at 1619 cm<sup>-1</sup> in the free ligand (**L**). This small spectral shift could be attributed to the coordination between the Ag(I) ion and the azine ligand via the N-atom of the C=N group. The  $\nu_{O-H}$  and  $\nu_{C=C}$  stretching vibrations appeared in both compounds at the same wavenumbers of 3432 and 1548 cm<sup>-1</sup>, respectively. An intense band appeared at 1384 cm<sup>-1</sup> only in the [Ag(L)(NO<sub>3</sub>)<sub>2</sub>] complex, corresponding to the  $\nu_{N-O}$  stretching vibration. This is good evidence of the presence of the nitrate group, which is not found in the FTIR spectra of the free ligand.



**Scheme 1.** Synthesis of the dinuclear Ag(I)-azine complex.

The X-ray photoelectron spectral analysis confirmed the elemental composition in  $[\text{Ag}(\text{L})(\text{NO}_3)_2]$  and highlighted the spin-orbital coupling for each element that is directly affected by their structure and oxidation states. Elemental composition and characteristic binding energies are reported in Table 1, while Figure 2 represents the binding energy–intensity relationship for Ag, N, S, O and C in the studied complex [34–36].

**Table 1.** Binding energies and chemical composition of  $[\text{Ag}(\text{L})(\text{NO}_3)_2]$ .

Name	Peak BE (eV)	Atomic %
C1s	284.68	21.45
C1s A	285.25	21.08
C1s B	286.29	18.25
O1s	532.60	18.34
N1s	399.78	7.91
N1s A	406.71	2.96
Ag3d, 5/2	368.49	3.95
Ag3d, 3/2	374.50	2.66
S2p, 3/2	164.76	1.97
S2p, 1/2	165.92	1.42

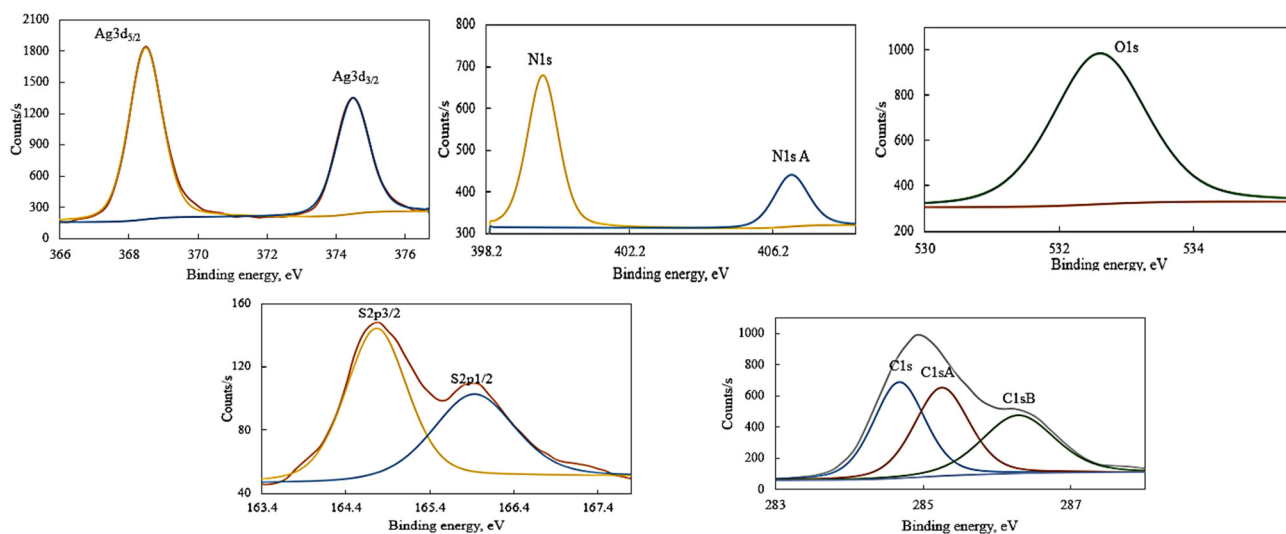


**Figure 2.** XPS spectra of Ag3d, N1s, O1s, S2p and C1s in  $[\text{Ag}(\text{L})(\text{NO}_3)_2]$  complex.

Silver showed a characteristic doublet peak corresponding to the Ag(I) oxidation state as  $3d_{3/2}$  and  $3d_{5/2}$  with binding energies (B.E) of 374.50 and 368.49 eV, respectively, with spin-orbit splitting  $\Delta E = 6.01$  eV and an intensity ratio of 0.67. Nitrogen showed two peaks: N1s at 399.78 eV for covalent-coordinate nitrogen atoms and a characteristic peak of nitrate nitrogen N1sA at 406.71 eV. Sulphur in the thiazolyl ring showed a characteristic doublet peak at 165.92 and 164.76 eV, corresponding to  $S2p_{5/2}$  and  $S2p_{3/2}$ , respectively, with  $\Delta E = 1.16$  eV and an intensity ratio of 0.55. Carbon showed three characteristic peaks as C1s, C1sA and C1sB at 284.68, 285.25 and 286.29 eV, respectively, confirming the presence of C-C, C-S and C-N/C-O bonds. Oxygen showed one broad peak centered at 532.6 eV.

## 2.2. X-ray Structure Description of $[\text{Ag}(\text{L})(\text{NO}_3)]_2$ Complex

The X-ray structure showing the asymmetric unit of the  $[\text{Ag}(\text{L})(\text{NO}_3)]_2$  complex is shown in the upper part of Figure 3. This complex was crystallized in the monoclinic crystal system and  $P2_1/n$  space group. The unit cell parameters were  $a = 10.3274(2)$  Å,  $b = 11.4504(3)$  Å,  $c = 12.7137(3)$  Å and  $\beta = 108.2560(10)^\circ$ . The asymmetric unit comprised one  $[\text{Ag}(\text{L})(\text{NO}_3)]$  formula. The azine ligand **L** and the nitrate group acted as bidentate chelates. The azine ligand **L** formed two significantly different interactions with Ag(I) via one nitrogen atom from the thiazole moiety and another nitrogen atom from one of the two N-atoms of the azine group. The Ag1-N1 and Ag1-N2 distances were 2.218(5) and 2.603(4) Å, respectively (Table 2). The bite angle of the azine ligand was  $69.37(16)^\circ$ . Additionally, the Ag1-O2 and Ag1-O3 bonds with the nitrate group were not equidistant. The former was significantly shorter (2.347(6) Å) than the latter (2.631(6) Å). The bite angle in this case was only  $50.4(2)^\circ$ . Interestingly, the Ag1 formed a weak interaction with a neighboring complex molecule via the symmetry related O3# atom, where the Ag1-O3# distance was found to be 2.781(7) Å. Hence, the molecular structure of this complex could be described by the dimeric structure  $[\text{Ag}(\text{L})(\text{NO}_3)]_2$  shown in the lower part of Figure 3. Thus, the Ag(I) was penta-coordinated with the  $\text{AgN}_2\text{O}_3$  coordination environment. The structure of the Ag(I) complex was found to be stabilized by the intramolecular O-H...N hydrogen bond occurring between the OH group as the hydrogen bond donor and the other freely uncoordinated nitrogen of the azine moiety (Figure 3, upper part). For better clarity, the intramolecular O-H...N hydrogen bond is illustrated as a turquoise dotted line in this part of Figure 3. The hydrogen-acceptor and donor-acceptor distances were 1.82(11) and 2.652(8) Å, respectively.

**Table 2.** The important geometric parameters in the  $[\text{Ag}(\text{L})(\text{NO}_3)]_2$  complex; the independent complex units are related by inversion center.

Bond	Distance (Å)	Bond(s)	Angle ( $^\circ$ )
Ag1-N1	2.218(5)	N1-Ag1-O2	156.3(2)
Ag1-O2	2.347(6)	N1-Ag1-N2	69.37(16)
Ag1-N2	2.603(4)	O2-Ag1-N2	95.65(17)
Ag1-O3	2.631(6)	O2-Ag1-O3	50.4(2)
Ag1-O3 #	2.781(7)	N2-Ag1-O3 #	164.8(2)
		O2-Ag1-O3 #	99.0(2)
		O3-Ag1-O3 #	79.2(2)

#  $2-x, 1-y, 1-z$ .

The packing of the  $[\text{Ag}(\text{L})(\text{NO}_3)]_2$  complex is dominated by the weak non-covalent C-H...O interactions, as depicted in Table 3 and shown as a red dotted line in the upper part of Figure 4. A view of the packing through the  $bc$  plane showing the complex units connected by the C-H...O interactions is presented in the lower part of the same illustration. The donor-acceptor interaction distances range from 3.149(8) Å (C1-H1A...O4) to 3.487(10) Å (C5-H5C...O4).

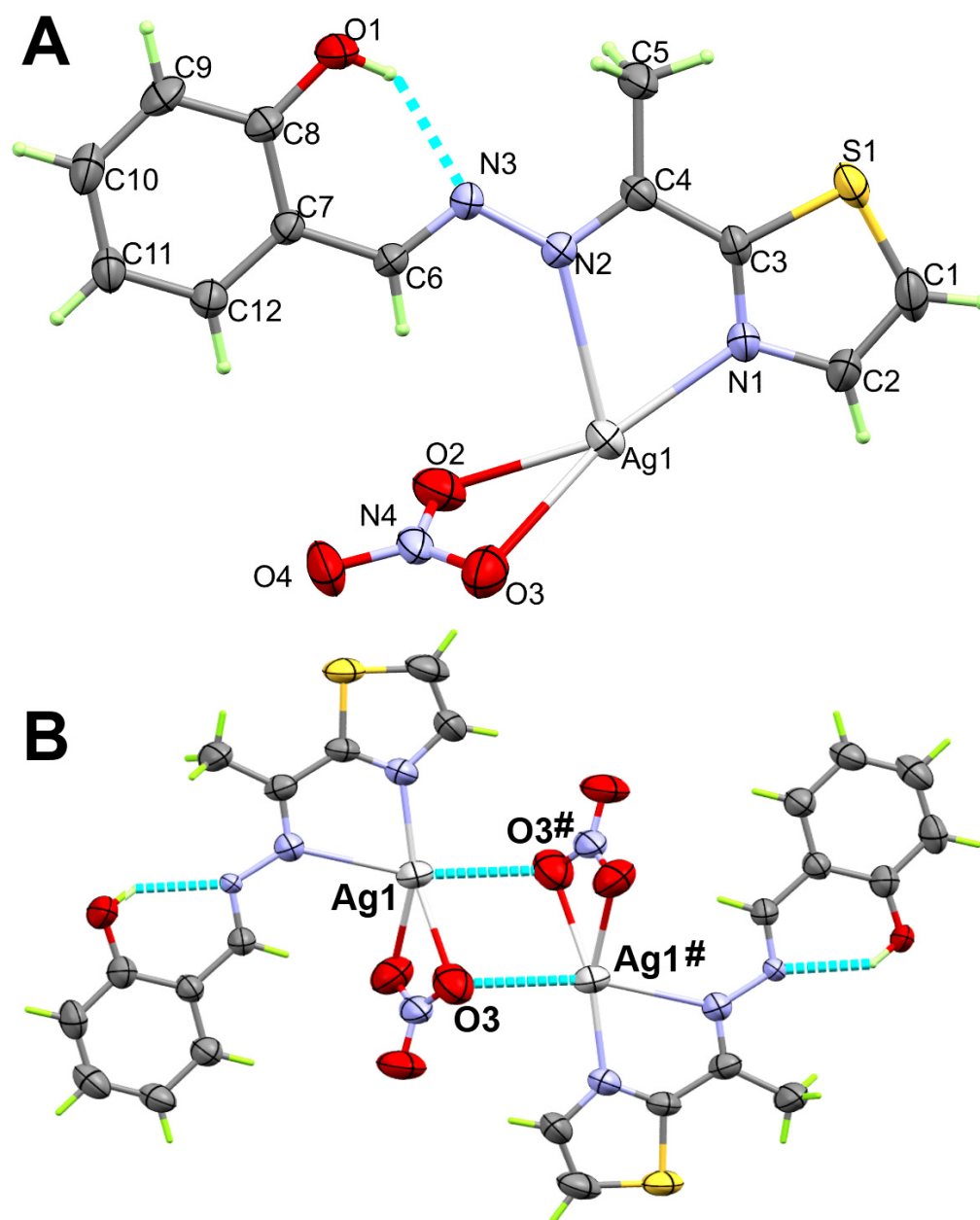


**Figure 3.** The asymmetric unit (A) and dinuclear formula (B) of the  $[\text{Ag}(\text{L})(\text{NO}_3)_2]$  complex. The symmetry code of  $\text{O}3^\#$  and  $\text{Ag}1^\#$  is  $2-x, 1-y, 1-z$ .

**Table 3.** Hydrogen bond parameters ( $\text{\AA}$ ,  $^\circ$ ) in  $[\text{Ag}(\text{L})(\text{NO}_3)_2]$  complex.

D-H...A	d(D-H)	d(H...A)	d(D...A)	$\angle(\text{DHA})$	Symm. Code
O1-H1...N3	0.91(11)	1.82(11)	2.652(8)	152(9)	
C1-H1A...O4	0.93	2.46	3.149(8)	131	$x, 1+y, z$
C5-H5A...O2	0.96	2.58	3.435(10)	149	$1-x, 1-y, 1-z$
C5-H5C...O4	0.96	2.59	3.487(10)	155	$3/2-x, 1/2+y, 3/2-z$

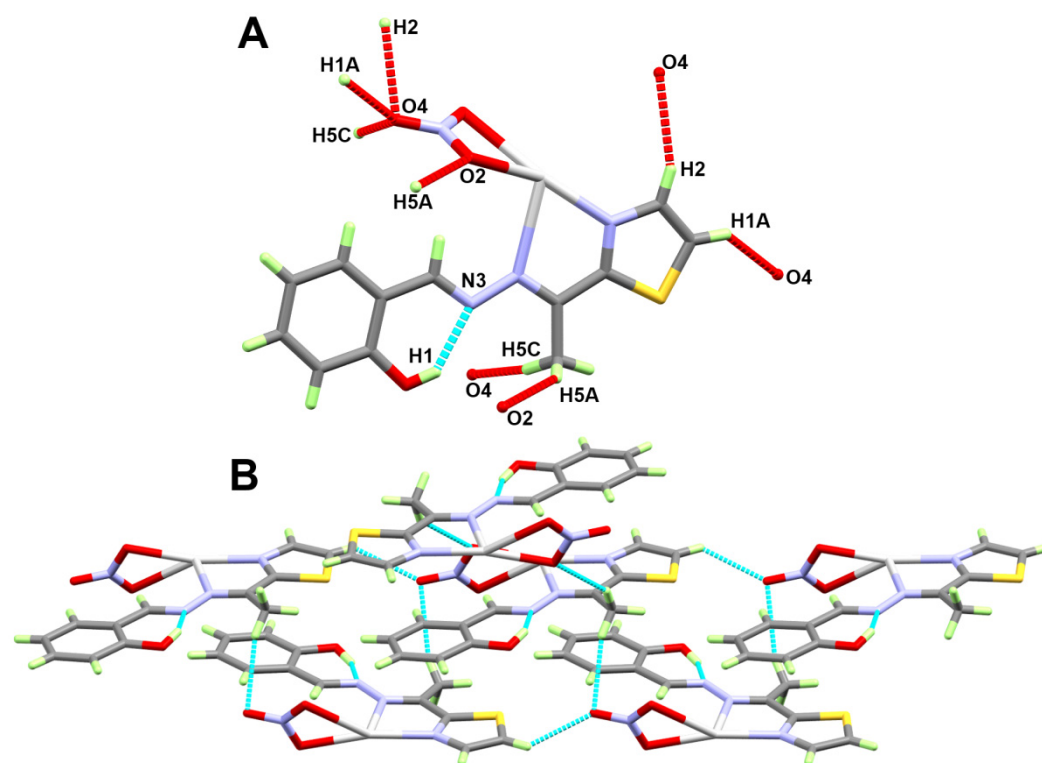


**Figure 4.** Intermolecular C-H ... O contacts (A) and packing scheme along *ab* plane (B) of the  $[\text{Ag}(\text{L})(\text{NO}_3)_2]$  complex. Symmetry codes are given in Table 3.

### 2.3. Hirshfeld Analysis

It is well acknowledged that the molecules in the crystal are packed in a way that maximizes the crystal stability via complicated sets of intermolecular interactions. Hirshfeld analysis is considered a powerful tool for predicting all intermolecular contacts in the crystal. For the  $[\text{Ag}(\text{L})(\text{NO}_3)_2]$  complex unit, the different Hirshfeld surfaces are shown in Figure 5. There are three Hirshfeld surfaces:  $d_{\text{norm}}$ , shape index and curvedness. According to Spackman et al., the  $d_{\text{norm}}$  is the normalized contact distance, shape index shows the shape of surface (concave  $(-1.0)$  to convex  $(+1.0)$ ) and curvedness indicates the surface flatness (flat  $(-4.0)$  to singular  $(+0.4)$ ) [37].

There are many red spots in the  $d_{\text{norm}}$  map, and these refer to the short distance Ag ... O, Ag ... C and O ... H contacts. The Ag1 ... C10 (3.389 Å) and Ag1 ... C11 (3.286 Å) as well as the O4 ... H1A (2.363 Å), O4 ... H5C (2.486 Å) and O4 ... H2 (2.375 Å) contacts have shorter distances than the vdWs radii sum of the interacting atoms. The red spots close to the Ag1 and O3 atoms are related to the weak Ag1-O3 bond (2.782 Å), which confirms the dinuclear formula of this complex. Additionally, the presence of red/blue triangles combination in the shape index as well as the flat green area in curvedness reveals the presence of some  $\pi$ - $\pi$  stacking interactions between the phenyl and thiazolyl aromatic moieties, where the shortest C ... C contact distance is 3.408 Å and corresponds to the C2 ... C10 contact. This interaction has a slightly longer distance than twice the vdWs radii of carbon atoms indicating relatively weak  $\pi$ - $\pi$  stacking interactions between the phenyl and thiazolyl moieties. The rings centroid-centroid distance was calculated to be 3.697 Å, which shows the importance of stacking interactions involving  $\pi$ -electrons of these aromatic rings in the molecular packing of the studied complex. All these interactions appeared as sharp spikes in the fingerprint plots, revealing short distances and strong interactions (Figure 6).

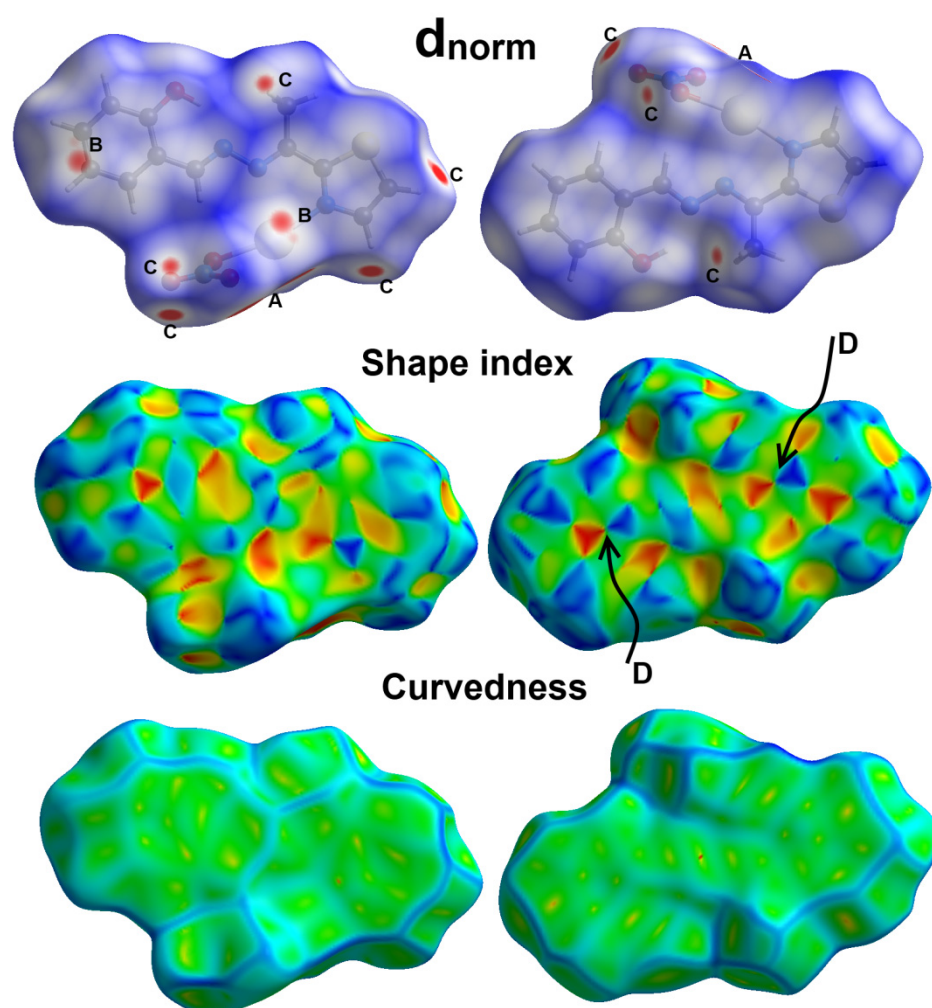


**Figure 5.** Hirshfeld surfaces for  $[\text{Ag}(\text{L})(\text{NO}_3)_2]$  complex. A, B, C and D refer to the Ag ... O, Ag ... C, O ... H and C ... C contacts, respectively.

Moreover, the Hirshfeld analysis gave accurate results for the percentages of the different intermolecular contacts between the surface and neighboring molecules (Figure 7). The most dominant contacts were the O ... H and H ... H interactions, which contributed to more than half of the whole observed contacts. Additionally, the percentage of Ag ... O, Ag ... C and C ... C interactions were 3.7, 2.9 and 6.7%, respectively. Other contacts shown in Figure 7 were less dominant in the molecular packing of the  $[\text{Ag}(\text{L})(\text{NO}_3)]$  complex. The interactions between all neighboring molecules and the surface are shown in Figure 8.

## 2.4. Biological Studies

### 2.4.1. Antimicrobial Activity

The antimicrobial activity of the studied Ag(I) complex on selected bacterial and fungal strains was determined in terms of the inhibition zone diameter (IZD) and the minimum inhibitory concentration (MIC). The antimicrobial activity results are depicted in Table 4. The IZDs are very small for the Gram-positive bacterial strain compared with Gram-negative bacteria. The sizes of the inhibition zones were 8 and 9 mm for *S. aureus* and *B. subtilis*, respectively, compared with 12 and 15 mm for *E. coli* and *P. vulgaris*, respectively. Hence, the studied Ag(I) complex is more potent against Gram-negative bacteria than Gram-positive bacteria. Moreover, the MIC value was lowest for *P. vulgaris* (625  $\mu\text{g}/\text{mL}$ ), which indicates the highest potency against this bacterium. In comparison with the antibacterial control Gentamycin, the studied Ag(I) complex is considered a weak antibacterial agent. In terms of antifungal activity, the studied  $[\text{Ag}(\text{L})(\text{NO}_3)_2]$  complex

inhibited both *A. fumigatus* and *C. albicans*. The IZDs were 31 and 18 mm for *A. fumigatus* and *C. albicans*, respectively, while the IZDs were 17 and 20 mm, respectively, for the standard Ketoconazole. The corresponding MIC values were 20, 625, 156 and 312  $\mu\text{g}/\text{mL}$ . Hence, the studied Ag(I) complex showed the highest potency against *A. fumigatus* compared with the other microbes.

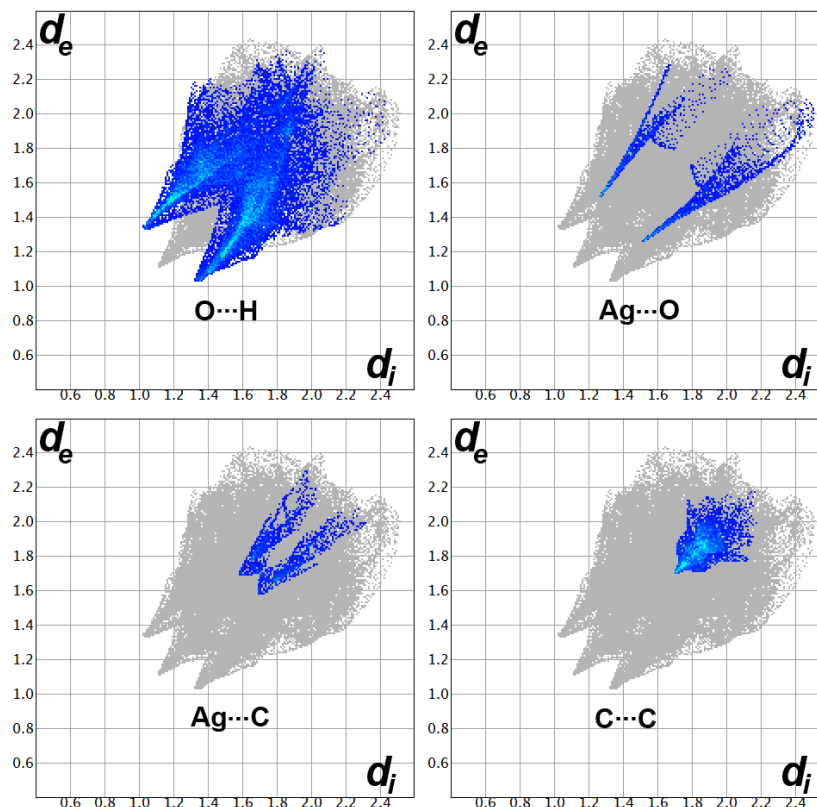


Figure 6. The decomposed fingerprint plots in  $[\text{Ag}(\text{L})(\text{NO}_3)]$  complex.

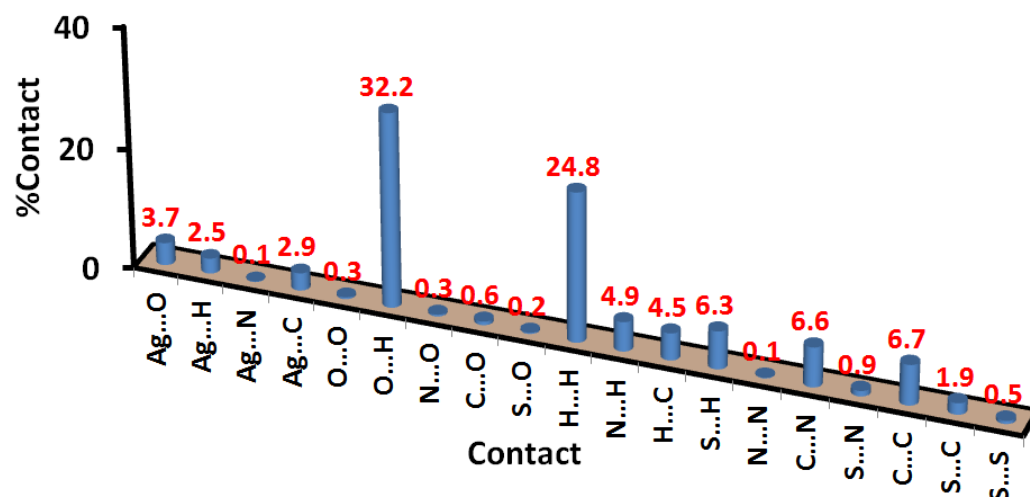
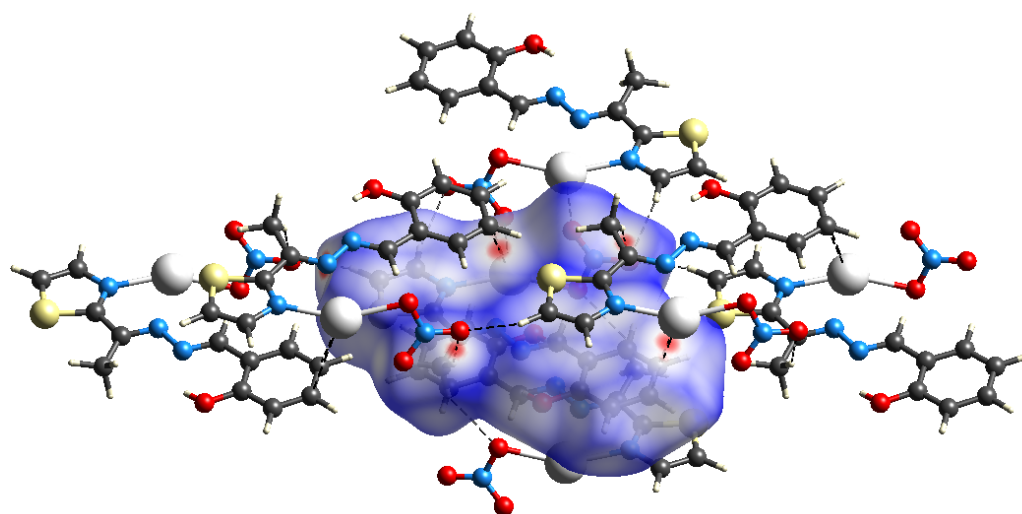


Figure 7. Percentages of all intermolecular contacts between the surface and neighboring molecules.



**Figure 8.** The interactions between the surface and neighboring molecules.

**Table 4.** IZDs (mm) and MICs ( $\mu\text{g}/\text{mL}$ ) for  $[\text{Ag}(\text{L})(\text{NO}_3)]_2$  complex <sup>a</sup>.

Microbe	$[\text{Ag}(\text{L})(\text{NO}_3)]_2$	Free L	Control
<i>A. fumigatus</i>	31 (20)	-	17(156) <sup>b</sup>
<i>C. albicans</i>	18 (625)	-	20(312) <sup>b</sup>
<i>S. aureus</i>	8 (5000)	11(1250)	24(10) <sup>c</sup>
<i>B. subtilis</i>	9 (5000)	-	26(5) <sup>c</sup>
<i>E. coli</i>	12 (1250)	-	30(5) <sup>c</sup>
<i>P. vulgaris</i>	15 (625)	-	25(5) <sup>c</sup>

<sup>a</sup> Values in parentheses for MIC, <sup>b</sup> Ketoconazole, <sup>c</sup> Gentamycin.

Additionally, the antimicrobial activities of the free L against the same microbes were examined, and the results were compared with those of the  $[\text{Ag}(\text{L})(\text{NO}_3)]_2$  complex (Table 4). It is clear that the free ligand (L) is active only against *S. aureus*. It has greater activity against this microbe than the  $[\text{Ag}(\text{L})(\text{NO}_3)]_2$  complex. The inhibition zone diameters are 8 and 11 mm, respectively. In contrast, the free ligand is not active at the applied concentration against any other microbe, while the  $[\text{Ag}(\text{L})(\text{NO}_3)]_2$  complex showed diverse antibacterial and antifungal activities.

#### 2.4.2. Anticancer and Antioxidant Activities

The results of the cytotoxicity test for the  $[\text{Ag}(\text{L})(\text{NO}_3)]_2$  complex against colon carcinoma are presented in Table 5. The %cell viability reached only  $1.28 \pm 0.46$  at  $500 \mu\text{g}/\text{mL}$ , and the concentration required to cause toxic effects in 50% of intact cells ( $\text{IC}_{50}$ ) was determined to be  $12.53 \pm 0.69 \mu\text{g}/\text{mL}$ . This indicates high cytotoxic activity against this cell line. For the free ligand (L), the  $\text{IC}_{50}$  value was determined to be  $242.92 \pm 8.12 \mu\text{g}/\text{mL}$ , which indicates lower cytotoxic effect of the free ligand and confirms the enhancement in cytotoxic activity as a result of the complexation between the ligand L and Ag(I) ion. The corresponding value for *cis*-platin as positive control was  $5.35 \pm 0.49 \mu\text{g}/\text{mL}$  in the same experimental conditions. Hence, the studied  $[\text{Ag}(\text{L})(\text{NO}_3)]_2$  complex has promising cytotoxic activity against the examined cell line.

The results of the antioxidant activity of the  $[\text{Ag}(\text{L})(\text{NO}_3)]_2$  complex, determined using the DPPH (2,2-diphenyl-1-picrylhydrazyl) assay [38], is reported in Table 6. The %DPPH scavenging at  $1280 \mu\text{g}/\text{mL}$  was only 75.18%, indicating low antioxidant activity of the  $[\text{Ag}(\text{L})(\text{NO}_3)]_2$  complex. Moreover, the concentration required to inhibit DPPH radical by 50% ( $\text{IC}_{50}$ ) was determined to be  $626.91 \pm 10.87 \mu\text{g}/\text{mL}$ , which further confirms the low antioxidant activity of the Ag(I) complex. The corresponding values for the free ligand L and ascorbic acid as positive control were  $156.48 \pm 3.66$  and  $12.3 \pm 0.51 \mu\text{g}/\text{mL}$ , respectively.

These results indicated low antioxidant activity of the  $[\text{Ag}(\text{L})(\text{NO}_3)]_2$  complex compared with the positive control and the free ligand.

**Table 5.** The cytotoxicity of  $[\text{Ag}(\text{L})(\text{NO}_3)]_2$  complex against colon carcinoma.

Sample Conc. ( $\mu\text{g}/\text{mL}$ )	Viability %	Inhibitory %	S.D. ( $\pm$ ) <sup>a</sup>
500	1.28	98.72	0.46
250	3.96	96.04	0.32
125	8.48	91.52	0.74
62.5	15.27	84.73	1.35
31.25	29.96	70.04	1.82
15.6	42.81	57.19	1.65
7.8	61.29	38.71	2.73
3.9	75.46	24.54	2.08
2	86.13	13.87	1.95
1	90.47	9.53	1.21
0	100	0	0

<sup>a</sup> Standard deviation.

**Table 6.** DPPH scavenging assay for  $[\text{Ag}(\text{L})(\text{NO}_3)]_2$  complex<sup>a</sup>.

Sample Conc. ( $\mu\text{g}/\text{mL}$ )	DPPH Scavenging %	S.D. ( $\pm$ )
1280	75.18	1.68
640	50.73	2.09
320	32.91	2.43
160	15.29	1.17
80	9.73	0.65
40	6.28	0.46
20	4.09	0.35
10	1.85	0.29
5	0.91	0.17
2.5	0.23	0.09
0	0	0

<sup>a</sup> Standard deviation.

### 3. Materials and Methods

#### 3.1. Materials

All chemicals were purchased from Aldrich chemical company.

#### 3.2. Instruments

Instruments including the X-ray diffractometer used for the single crystal structure measurement and solution structure details [39,40] are given in the Supplementary Data. The crystallographic data of the  $[\text{Ag}(\text{L})(\text{NO}_3)]_2$  complex are listed in Table 7.

#### 3.3. Synthesis of $[\text{Ag}(\text{L})(\text{NO}_3)]_2$ Complex

The azine ligand (**L**) was synthesized using the method described in the Supplementary Data and following procedures present in the literature [41,42]. An ethanolic solution of **L** (0.1 mmol in 10 mL) was added to 0.1 mmol of  $\text{AgNO}_3$  in 5 mL of distilled water. An immediate yellow precipitate was formed, which was dissolved by adding 5 mL of acetonitrile. The solution was filtered, and the clear solution was then left at room temperature to slowly evaporate. After 5 days, a yellow crystalline product was obtained for the  $[\text{Ag}(\text{L})(\text{NO}_3)]_2$  complex (Yield: 76%).

Anal. Calc. for  $\text{C}_{24}\text{H}_{22}\text{Ag}_2\text{N}_8\text{O}_8\text{S}_2$ : C, 34.72; H, 2.67; N, 13.49; Ag, 25.98%. Found: C, 34.56; H, 2.58; N, 13.33; Ag, 25.72%. IR (KBr,  $\text{cm}^{-1}$ ): 3432, 1615, 1548, 1384.

#### 3.4. Hirshfeld Calculations

The Hirshfeld topology analyses were performed using the crystal explorer 17.5 program [37].

**Table 7.** Crystal data of [Ag(L)(NO<sub>3</sub>)<sub>2</sub>] complex.

CCDC	2207716
Empirical formula	C <sub>24</sub> H <sub>22</sub> Ag <sub>2</sub> N <sub>8</sub> O <sub>8</sub> S <sub>2</sub>
Fw	830.35 g/mol
Temp	296(2) K
λ	1.54178 Å
cryst syst	Monoclinic
Space group	P2 <sub>1</sub> /n
a/Å	10.3274(2) Å
b/Å	11.4504(3) Å
c/Å	12.7137(3) Å
α/°	90°
β/°	108.2560(10)°
γ/°	90°
V	1427.76(6) Å <sup>3</sup>
Z	2
ρ <sub>calc</sub>	1.931 g/cm <sup>3</sup>
μ(Cu Kα)	12.933 mm <sup>-1</sup>
Reflections collected	15004
Independent reflections	2487 [R(int) = 0.0628]
Completeness to theta = 66.67°	98.6%
Data/restraints/parameters	2487/0/204
GOOF (F <sup>2</sup> )	1.094
Final R indices [I > 2sigma(I)]	R <sub>1</sub> = 0.0595, wR <sub>2</sub> = 0.1687
R indices (all data)	R <sub>1</sub> = 0.0662, wR <sub>2</sub> = 0.1793
Largest diff. peak and hole	1.574 and −1.154

### 3.5. Biological Studies

The bioactivities of the [Ag(L)(NO<sub>3</sub>)<sub>2</sub>] complex were determined according to the biological activity methods listed in the Supplementary Data [38,43,44].

## 4. Conclusions

A new dinuclear [Ag(L)(NO<sub>3</sub>)<sub>2</sub>] complex of the asymmetric azine-type ligand (L) was synthesized by a self-assembly method. The azine ligand L acts as a bidentate chelate via the thiazole and azine nitrogen atoms. Additionally, the nitrate ion is a bidentate ligand via two non-equidistant Ag–O bonds. The bite angles of the two bidentate chelates are 69.37(16)° and 50.4(2)°, respectively. The coordination sphere of Ag(I) is completed by one weak Ag–O bond with an oxygen atom from a neighboring nitrate group in another [Ag(L)(NO<sub>3</sub>)] unit. Hence, the coordination number of the silver is five, and the structure could be represented by the dinuclear formula [Ag(L)(NO<sub>3</sub>)<sub>2</sub>]. Hirshfeld analysis of the [Ag(L)(NO<sub>3</sub>)] complex revealed the importance of the Ag ... C, O ... H and C ... C contacts in molecular packing. The studied Ag(I) complex showed promising antifungal activity against *A. fumigatus*. Although the studied Ag(I) complex showed very weak antioxidant activity, the cytotoxicity results were promising. The IC<sub>50</sub> value against colon carcinoma (HCT-116 cell line) was determined to be 12.53 ± 0.69 μg/mL, which is compared with 5.35 ± 0.49 μg/mL for *cis*-platin. In comparison with the free ligand, the Ag(I) complex has higher cytotoxicity (242.92 ± 8.12 μg/mL). Additionally, the Ag(I) complex has greater antimicrobial activity than the free ligand against all microbes except *S. aureus*.

**Supplementary Materials:** The following supporting information can be downloaded at: <https://www.mdpi.com/article/10.3390/inorganics10110209/s1>; Figure S1, FTIR spectra of L (upper) and [Ag(L)(NO<sub>3</sub>)<sub>2</sub>] (lower) complex; Figure S2, NMR spectra of L; instrumental details; biological activity methods and synthesis of L; Table S1, the cytotoxicity of the free ligand (L) against colon carcinoma; Table S2, DPPH scavenging assay for of the free ligand (L).

**Author Contributions:** Conceptualization, S.M.S., A.E.A. and H.A.E.; methodology, H.A.E. and S.M.S.; software, S.M.S., M.S.A. and H.A.E.; formal analysis, S.M.S., H.A.E., D.A.-W. and A.B.; investigation, H.A.E. and S.M.S.; resources, H.A.E., A.E.A., A.B. and M.S.A.; funding acquisition: M.S.A. and A.B.; writing—original draft preparation, H.A.E., A.E.A., A.B. and D.A.-W.; writing—review and editing, H.A.E., A.E.A., A.B., D.A.-W. and S.M.S.; supervision, S.M.S., A.E.A. and H.A.E. All authors have read and agreed to the published version of the manuscript.

**Funding:** Princess Nourah bint Abdulrahman University Researchers Supporting Project number (PNURSP2022R86), Princess Nourah bint Abdulrahman University, Riyadh, Saudi Arabia.

**Institutional Review Board Statement:** Not applicable.

**Informed Consent Statement:** Not applicable.

**Data Availability Statement:** Not applicable.

**Acknowledgments:** Princess Nourah bint Abdulrahman University Researchers Supporting Project number (PNURSP2022R86), Princess Nourah bint Abdulrahman University, Riyadh, Saudi Arabia. We would also like to acknowledge the general facility at the College of Science-Kuwait University for obtaining the X-ray crystallography measurements and XPS measurements via the general facility project No. GS 03/08 and GS01/05. Special thanks to Mickey Vinodh (Kuwait University-College of Science-General Facility) for his assistance in the processing of the X-ray data and Ahmed Meslam (Kuwait University-College of Science-General Facility) for his assistance in obtaining the XPS data.

**Conflicts of Interest:** The authors declare no conflict of interest.

## References

1. Adsule, S.; Barve, V.; Chen, D.; Ahmed, F.; Dou, Q.P.; Padhye, S.; Sarkar, F.H. Novel Schiff base copper complexes of quinoline-2 carboxaldehyde as proteasome inhibitors in human prostate cancer cells. *J. Med. Chem.* **2006**, *49*, 7242–7246. [[CrossRef](#)] [[PubMed](#)]
2. Weber, B.; Serafin, A.; Michie, J.; Van Rensburg, C.; Swarts, J.; Bohm, L. Cytotoxicity and cell death pathways invoked by two new rhodium-ferrocene complexes in benign and malignant prostatic cell lines. *Anticancer Res.* **2004**, *24*, 763–770. [[PubMed](#)]
3. Shago, R.F.; Swarts, J.C.; Kreft, E.; Van Rensburg, C.E. Antineoplastic activity of a series of ferrocene-containing alcohols. *Anticancer Res.* **2007**, *27*, 3431–3433. [[PubMed](#)]
4. Basu Baul, T.S.; Basu, S.; de Vos, D.; Linden, A. Amino acetate functionalized Schiff base organotin (IV) complexes as anticancer drugs: Synthesis, structural characterization, and in vitro cytotoxicity studies. *Investig. New Drugs* **2009**, *27*, 419–431. [[CrossRef](#)]
5. Chan, M.-H.E.; Crouse, K.A.; Tahir, M.I.M.; Rosli, R.; Umar-Tsafe, N.; Cowley, A.R. Synthesis and characterization of cobalt (II), nickel (II), copper (II), zinc (II) and cadmium (II) complexes of benzyl N-[1-(thiophen-2-yl) ethylidene] hydrazine carbodithioate and benzyl N-[1-(thiophen-3-yl) ethylidene] hydrazine carbodithioate and the X-ray crystal structure of bis nickel (II). *Polyhedron* **2008**, *27*, 1141–1149.
6. Zhang, C.X.; Lippard, S.J. New metal complexes as potential therapeutics. *Curr. Opin. Chem. Biol.* **2003**, *7*, 481–489. [[CrossRef](#)]
7. Ott, I. On the medicinal chemistry of gold complexes as anticancer drugs. *Coord. Chem. Rev.* **2009**, *253*, 1670–1681. [[CrossRef](#)]
8. Berners-Price, S.J.; Johnson, R.K.; Giovenella, A.J.; Faucette, L.F.; Mirabelli, C.K.; Sadler, P.J. Antimicrobial and anticancer activity of tetrahedral, chelated, diphosphine silver (I) complexes: Comparison with copper and gold. *J. Inorg. Biochem.* **1988**, *33*, 285–295. [[CrossRef](#)]
9. Zartilas, S.; Hadjikakou, S.K.; Hadjiliadis, N.; Kourkoumelis, N.; Kyros, L.; Kubicki, M.; Baril, M.; Butler, I.S.; Karkabounas, S.; Balzarini, J. Tetrameric 1: 1 and monomeric 1: 3 complexes of silver (I) halides with tri (p-tolyl)-phosphine: A structural and biological study. *Inorg. Chim. Acta* **2009**, *362*, 1003–1010. [[CrossRef](#)]
10. Liu, J.J.; Galettis, P.; Farr, A.; Maharaj, L.; Samarasingha, H.; McGechan, A.C.; Baguley, B.C.; Bowen, R.J.; Berners-Price, S.J.; McKeage, M.J. In vitro antitumour and hepatotoxicity profiles of Au (I) and Ag (I) bidentate pyridyl phosphine complexes and relationships to cellular uptake. *J. Inorg. Biochem.* **2008**, *102*, 303–310. [[CrossRef](#)]
11. Teyssot, M.-L.; Jarrousse, A.-S.; Manin, M.; Chevry, A.; Roche, S.; Norre, F.; Beaudoin, C.; Morel, L.; Boyer, D.; Mahiou, R. Metal-NHC complexes: A survey of anti-cancer properties. *Dalton Trans.* **2009**, *35*, 6894–6902. [[CrossRef](#)] [[PubMed](#)]
12. Zhu, H.-L.; Zhang, X.-M.; Liu, X.-Y.; Wang, X.-J.; Liu, G.-F.; Usman, A.; Fun, H.-K. Clear Ag–Ag bonds in three silver (I) carboxylate complexes with high cytotoxicity properties. *Inorg. Chem. Commun.* **2003**, *6*, 1113–1116. [[CrossRef](#)]
13. Patil, S.; Claffey, J.; Deally, A.; Hogan, M.; Gleeson, B.; Menéndez Méndez, L.M.; Müller-Bunz, H.; Paradisi, F.; Tacke, M. *Synthesis, Cytotoxicity and Antibacterial Studies of p-Methoxybenzyl-Substituted and Benzyl-Substituted N-Heterocyclic Carbene–Silver Complexes*; Wiley Online Library: New York, NJ, USA, 2010.
14. Siciliano, T.J.; Deblock, M.C.; Hindi, K.M.; Durmus, S.; Panzner, M.J.; Tessier, C.A.; Youngs, W.J. Synthesis and anticancer properties of gold (I) and silver (I) N-heterocyclic carbene complexes. *J. Organomet. Chem.* **2011**, *696*, 1066–1071. [[CrossRef](#)]
15. Ivanova, B.; Spitteller, M. Coordination ability of silver (I) with antimycins and actinomycins—Properties of the T-shaped chromophores. *Polyhedron* **2012**, *38*, 235–244. [[CrossRef](#)]

16. Pandeya, S.; Sriram, D.; Nath, G.; DeClercq, E. Synthesis, antibacterial, antifungal and anti-HIV activities of Schiff and Mannich bases derived from isatin derivatives and N-[4-(4'-chlorophenyl) thiazol-2-yl] thiosemicarbazide. *Eur. J. Pharm. Sci.* **1999**, *9*, 25–31. [[CrossRef](#)]
17. Chen, H.; Rhodes, J. Schiff base forming drugs: Mechanisms of immune potentiation and therapeutic potential. *J. Mol. Med.* **1996**, *74*, 497–504. [[CrossRef](#)]
18. Sakiyan, I.; Logoglu, E.; Arslan, S.; Sari, N.; Şakiyan, N. Antimicrobial activities of N-(2-hydroxy-1-naphthalidene)-amino acid (glycine, alanine, phenylalanine, histidine, tryptophane) Schiff bases and their manganese (III) complexes. *Biomaterials* **2004**, *17*, 115–120. [[CrossRef](#)]
19. Holla, B.S.; Rao, B.S.; Shridhara, K.; Akberali, P. Studies on arylfuran derivatives: Part XI. Synthesis, characterisation and biological studies on some Mannich bases carrying 2, 4-dichlorophenylfurfural moiety. *Il Farmaco* **2000**, *55*, 338–344. [[CrossRef](#)]
20. Hearn, M.J.; Cynamon, M.H.; Chen, M.F.; Coppins, R.; Davis, J.; Kang, H.J.-O.; Noble, A.; Tu-Sekine, B.; Terrot, M.S.; Trombino, D. Preparation and antitubercular activities in vitro and in vivo of novel Schiff bases of isoniazid. *Eur. J. Med. Chem.* **2009**, *44*, 4169–4178. [[CrossRef](#)]
21. Abu-Dief, A.M.; Mohamed, I.M. A review on versatile applications of transition metal complexes incorporating Schiff bases. *Beni-Suef Univ. J. Basic Appl. Sci.* **2015**, *4*, 119–133. [[CrossRef](#)]
22. Ali, M.; Jesmin, M.; Salahuddin, M.; Habib, M.; Khanam, J. Antineoplastic activity of N-salicylidene-glycinato-di-aquanickel (II) complex against Ehrlich Ascites Carcinoma (EAC) cells in mice. *Int. J. Biol. Chem. Sci.* **2008**, *2*, 292–298. [[CrossRef](#)]
23. Ali, M.A.; Haroon, C.M.; Nazimuddin, M.; Majumder, S.; Tarafder, M.T.; Khair, M.A. Synthesis, characterization and biological activities of some new nickel (II), copper (II), zinc (II) and cadmium (II) complexes of quadridentate SNNS ligands. *Transit. Met. Chem.* **1992**, *17*, 133–136. [[CrossRef](#)]
24. Hossain, M.E.; Alam, M.N.; Ali, M.A.; Nazimuddin, M.; Smith, F.E.; Hynes, R.C. The synthesis, characterization and bioactivities of some copper (II) complexes of the 2-acetylpyridine Schiff bases of s-methyl- and s-benzyl-dithiocarbamate, and the x-ray crystal structure of the nitrate (s-benzyl-β-n-(2-acetylpyridyl) methylenedithiocarbamate) copper (II) complex. *Polyhedron* **1996**, *15*, 973–980.
25. Hossain, M.E.; Alam, M.; Begum, J.; Ali, M.A.; Nazimuddin, M.; Smith, F.; Hynes, R. The preparation, characterization, crystal structure and biological activities of some copper (II) complexes of the 2-benzoylpyridine Schiff bases of S-methyl- and S-benzyl-dithiocarbamate. *Inorg. Chim. Acta* **1996**, *249*, 207–213. [[CrossRef](#)]
26. Wang, Q.; Yuen, M.C.W.; Lu, G.L.; Ho, C.L.; Zhou, G.J.; Keung, O.M.; Lam, K.H.; Gambari, R.; Tao, X.M.; Wong, R.S.M. Synthesis of 9, 9-Dialkyl-4, 5-diazafluorene Derivatives and Their Structure–Activity Relationships Toward Human Carcinoma Cell Lines. *ChemMedChem Chem. Enabling Drug Discov.* **2010**, *5*, 559–566. [[CrossRef](#)]
27. Constable, E.C.; Steel, P.J. N, N'-Chelating biheteroaromatic ligands; a survey. *Coord. Chem. Rev.* **1989**, *93*, 205–223. [[CrossRef](#)]
28. Yamamoto, T.; Zhou, Z.-h.; Kanbara, T.; Shimura, M.; Kizu, K.; Maruyama, T.; Nakamura, Y.; Fukuda, T.; Lee, B.-L.; Ooba, N. π-conjugated donor–acceptor copolymers constituted of π-excessive and π-deficient arylene units. Optical and electrochemical properties in relation to CT structure of the polymer. *J. Am. Chem. Soc.* **1996**, *118*, 10389–10399. [[CrossRef](#)]
29. Prasad, K.T.; Gupta, G.; Rao, A.V.; Das, B.; Rao, K.M. New series of platinum group metal complexes bearing η<sup>5</sup>- and η<sup>6</sup>-cyclichydrocarbons and Schiff base derived from 2-acetylthiazole: Syntheses and structural studies. *Polyhedron* **2009**, *28*, 2649–2654. [[CrossRef](#)]
30. Tan, X.-J.; Liu, H.-Z.; Ye, C.-Z.; Lou, J.-F.; Liu, Y.; Xing, D.-X.; Li, S.-P.; Liu, S.-L.; Song, L.-Z. Synthesis, characterization and in vitro cytotoxic properties of new silver (I) complexes of two novel Schiff bases derived from thiazole and pyrazine. *Polyhedron* **2014**, *71*, 119–132. [[CrossRef](#)]
31. Rogovoy, M.I.; Tomilenko, A.V.; Samsonenko, D.G.; Nedolya, N.A.; Rakhmanova, M.I.; Artem'ev, A.V. New silver (I) thiazole-based coordination polymers: Structural and photophysical investigation. *Mendeleev Commun.* **2020**, *30*, 728–730. [[CrossRef](#)]
32. Soliman, S.M.; Albering, J.H.; Barakat, A. Unexpected formation of polymeric silver (I) complexes of azine-type ligand via self-assembly of Ag-salts with isatin oxamohydrazide. *R. Soc. Open Sci.* **2018**, *5*, 180434. [[CrossRef](#)] [[PubMed](#)]
33. Soliman, S.M.; Barakat, A. Self-assembly of azine-based hydrolysis of pyridine and isatin oxamohydrazides with AgNO<sub>3</sub>; synthesis and structural studies of a novel four coordinated Ag (I)-azine 2D coordination polymer. *Inorg. Chim. Acta* **2019**, *490*, 227–234. [[CrossRef](#)]
34. Elbadawy, H.A.; Khalil, S.M.; Al-Wahaib, D.; Barakat, A.; Soliman, S.M.; Eldissouky, A. Ag (I)-mediated hydrolysis of hydrazone to azine: Synthesis, X-ray structure, and biological investigations of two new Ag (I)-azine complexes. *Appl. Organomet. Chem.* **2022**, *36*, e6757. [[CrossRef](#)]
35. Ferraria, A.M.; Carapeto, A.P.; do Rego, A.M.B. X-ray photoelectron spectroscopy: Silver salts revisited. *Vacuum* **2012**, *86*, 1988–1991. [[CrossRef](#)]
36. Volkov, I.L.; Smirnova, A.; Makarova, A.A.; Reveguk, Z.V.; Ramazanov, R.R.; Usachov, D.Y.; Adamchuk, V.K.; Kononov, A.I. DNA with ionic, atomic, and clustered silver: An XPS study. *J. Phys. Chem. B* **2017**, *121*, 2400–2406. [[CrossRef](#)]
37. Spackman, P.R.; Turner, M.J.; McKinnon, J.J.; Wolff, S.K.; Grimwood, D.J.; Jayatilaka, D.; Spackman, M.A. CrystalExplorer: A program for Hirshfeld surface analysis, visualization and quantitative analysis of molecular crystals. *J. Appl. Crystallogr.* **2021**, *54*, 1006–1011. [[CrossRef](#)] [[PubMed](#)]
38. Yen, G.C.; Duh, P.D. Scavenging effect of methanolic extracts of peanut hulls on free-radical and active-oxygen species. *J. Agric. Food Chem.* **1994**, *42*, 629–632. [[CrossRef](#)]

39. Sheldrick, G.M. SHELXT—Integrated space-group and crystal-structure determination. *Acta Crystallogr. Sect. A Found. Adv.* **2015**, *71*, 3–8. [[CrossRef](#)] [[PubMed](#)]
40. Sheldrick, G.M. Crystal structure refinement with SHELXL. *Acta Crystallogr. Sect. C Struct. Chem.* **2015**, *71*, 3–8. [[CrossRef](#)]
41. El-Faham, A.; Soliman, S.M.; Ghabbour, H.A.; Elnakady, Y.A.; Mohaya, T.A.; Siddiqui, M.R.; Albericio, F. Ultrasonic promoted synthesis of novel s-triazine-Schiff base derivatives; molecular structure, spectroscopic studies and their preliminary anti-proliferative activities. *J. Mol. Struct.* **2016**, *1125*, 121–135. [[CrossRef](#)]
42. Shang, Y.-F.; Wang, Q.-M.; Zhu, M.-L.; Zhang, Y.-H. 2-(Hydrazonomethyl) phenol. *Acta Crystallogr. Sect. E Struct. Rep. Online* **2009**, *65*, o3023. [[CrossRef](#)] [[PubMed](#)]
43. Cockerill, F. *Performance Standards for Antimicrobial Susceptibility Testing: Twenty-First Informational Supplement*; CLSI supplement M100–M121; Clinical and Laboratory Standards Institute: Wayne, PA, USA, 2012.
44. Mosmann, T. Rapid colorimetric assay for cellular growth and survival: Application to proliferation and cytotoxicity assays. *J. Immunol. Methods* **1983**, *65*, 55–63. [[CrossRef](#)]